Shahid et al., J Material Sci Eng 2016, 5:6
DOI: 10.4172/2169-0022.1000287

Journal of Material Sciences & Engineering

Research Article Open Access

Synthesis of Pyramid-Shaped NiO Nanostructures using Low-Temperature Composite- Hydroxide- Mediated Approach

Shahid T[2], Khan TM[1]*, Zakria M[1], Shakoor RI[1,4], Arfan M[2] and Khursheed S[2]

[1]National Institute of Lasers and Optronics (NILOP), Islamabad, Pakistan
[2]Department of Applied Physics, Federal Urdu University of Arts, Science and Technology, Islamabad, Pakistan
[3]School of Physics, Trinity College Dublin (TCD), Ireland
[4]Department of Mechanical Engineering, Muhammad Ali Jinnah University, Islamabad, Pakistan

Abstract

Composite-hydroxide-mediated (CHM) approach was used to synthesize NiO nanocrystals. The proposed method makes use of molten composite hydroxides; providing reaction media and lower the process temperature. Processing temperature and reaction time are the two potential parameters to control the growth of a nanomaterial. The method was used at temperatures in the range of 180-250°C and formation of the nanomaterial was monitored using XRD, SEM, EDX, FTIR, and UV-visible spectroscopy. The produced nanomaterial was purely polycrystalline with an average crystallite size in the range of 23.71-36.92 nm. Method suggested formation of pyramid shaped NiO nanocrystals in the temperature range 220-250°C. Evidence on the elemental composition, purity, and chemical bonding were obtained from EDX and FTIR analysis respectively. Estimation on direct bandgap was made from the optical analysis and found to be in the range 4.0-4.8 eV. The method is attractive and seems a cost effective route for the growth of transition metal oxides for research purpose. For further efficacy, the approach can be examined for other technologically significant nanostructures.

Keywords: CHM; Nanopyramids; NiO; SEM; Optical properties

Introduction

Nanotechnology has emerged potentially a versatile and interdisciplinary field involving many subjects of science and engineering; leading to a wide-range of new developments, innovation, and advanced significant research. Past few years are witnessed major mechanical advancements which are based on remarkable nanostructures level progress. Also, metal oxide nanomaterials including nanoparticles (NPs), nanowires, nanosheets, and nanofibers, has got an expanding attention of scientific researchers due to their potential applications in biomedical, optical, and electronic fields [1].

In the transition metal oxides, nickel oxide (NiO) is potentially important with a cubic lattice structure. It is a *p*-type semiconductor with a wide bandgap ranging from 3.6 eV to 4.0 eV. Recently, efforts have been placed to develop, characterize and describe the physio- chemical properties of NiO nanostructures. NiO has a number of intensive applications generally a pure material for specialty applications and metallurgical grade; mainly used for the manufacturing of alloys, frits, ferrites, porcelain glazes [2,3], magnetic materials [4], alkaline batteries cathode [5], anode material for Li-ion batteries [6,7], gas sensors [8], anti-ferromagnetic layers [9], solid-oxide fuel cells [10,11], drug delivery and magnetic resonance imaging (MRI) [12]. NiO use in nanoscale optoelectronics devices such as electrochromic display optical fibers, photovoltaic applications [13,14], p–n heterojunctions [15], catalysis [16,17], the electrode material for electrochemical capacitors, [18] and smart windows [19]. The requirements of these applications include many factors regarding small size and particle distribution. The factors include volume effect, the quantum size effect and the surface effect with improved properties for these various attractive applications [20]. In the literature, various methods have been reported for the synthesis of nanocrystalline NiO from different starting materials for some valuable applications. Most of these methods are; thermal decomposition [21,22], carbonyl method, sol-gel technique [23], microwave pyrolysis [24], solvothermal [25], anodic arc plasma [26], Sonochemical [27], precipitation-calcination [28] and microemulsion [29]. However, mostly these are high-temperature and high-pressure methods; rely on surface-capping agents or demand for organic-metallic precursors and seems to be expensive for an industrial scale application. So it is always desired to seek for a simple approach to be; cost effective, workable at lower temperature, and has potential for a large-scale and controlled growth of oxide nanostructures at atmospheric pressure.

The method we have proposed here for the preparation of NiO nanomaterial is the composite- hydroxide- mediated (CHM) approach. The method of CHM is basically a technically sound, environmentally friendly methodology for creating a wide range of significant nanostructures [30]. The method is quite cheap and single step technique provides a fast nano synthesis route for nanomaterials. The synthesis is usually carried out at a lower temperature ~200°C in the ambient atmosphere [30,31]. This method has the advantages to synthesize functional nanowires, nanorods, nanobelts and several other oxide nanostructures. Recently, Khan et al. applied this method for the synthesis of CdO and ZnO nanostructures and a temperature dependent study was established [32,33]. Previously in our group, a comprehensive study was done on the feasibility of CHM approach for the synthesis of doped $Cu_{1-x}Zn_xO$ nanostructures [34]. Interesting nanostructures with flower- like features and morphological peculiarities were obtained. These structures seem to strongly depend on the content of the incorporated Zn^{+2}. Recently, C An et al. applied

***Corresponding author:** Khan TM, National Institute of Lasers and Optronics (NILOP), Nilore 45650, Islamabad, Pakistan, Tel: 92-51-9248801; Fax: 92512208051; E-mail: tajakashne@gmail.com

Received August 29, 2016; **Accepted** October 04, 2016; **Published** October 14, 2016

Citation: Shahid T, Khan TM, Zakria M, Shakoor RI, Arfan M, et al. (2016) Synthesis of Pyramid-Shaped NiO Nanostructures using Low-Temperature Composite-Hydroxide- Mediated Approach. J Material Sci Eng 5: 287. doi:10.4172/2169-0022.1000287

this method to prepare NiO nanocrystals using $NiCl_2.6H_2O$ as the source material. However, in their limited study, they showed the dependence of synthesis process on the amount of solvents used with no further understanding of optical and morphological structures [35]. The method of CHM is extensively under investigation in direction of basic understanding for research purposes. The method seems has a potential to be a viable synthesis route for the high- tech industrial scale application if it is established.

In this report we present synthesis of purely NiO nanocrystals using a cost effective CHM approach and formation of the nanostructures is established using; X-ray diffraction (XRD), Fourier-transform infrared spectroscopy (FT-IR), UV-Visible spectroscopy, scanning electron microscopy (SEM), and energy dispersive x-ray spectroscopy (EDXS). We established that well defined interesting pyramid type nanocrystals are obtained in a certain temperature range and showed a temperature-dependent mechanism of the nanostructures. This study will help to understand and control morphology of the nanomaterial with the processing temperature. The proposed approach seems to provide a fast and cheap nano-synthesis route for a verity of novel nanomaterials of technological importance for research purposes.

Experimental Methods

Synthesis of NiO nanomaterial

The synthesis of NiO was performed using CHM approach. All the chemicals were the analytical grade, used without further purification and purchased from Merk Co. The main source materials used for this experiment are; Ni $(NO_3)_2.6H_2O$, NaOH, and KOH. The synthesis procedure has been given in our previous reports [32-34]. Briefly, for the synthesis of NiO, an appropriate amount of mixed hydroxide (NaOH: KOH=51.5:48.5) were added in a Teflon beaker, and covered beaker was then placed in an electric furnace at 180°C followed by further experiments at temperatures; 200°C, 220°C, and 250°C. Until the hydroxides were totally in the molten state, the beaker was taken out from the furnace. The molten hydroxide mixture was stirred well by a Teflon bar and Ni $(NO_3)_2.6H_2O$ was added. Then Teflon beaker was put in the furnace for 24 h (processing time) at the above- described temperatures for various repeated experiments. After a reaction time of 24 h, the beaker was taken out and cooled to room temperature naturally. The product was washed with distilled water to remove the hydroxide. The black powder was obtained and collected for further characterization. A general sketch showing the procedure of the process is given in Figure 1.

The reaction mechanism to form NiO nanocrystals can be formulated as follow:

$$Ni(NO_3).6H_2O + 2NaOH \rightarrow Ni(OH)2 + 2NaNO_3 + 6H_2O$$

$$\Rightarrow Ni^{2+} + 2OH^- \rightarrow Ni(OH)$$

$Ni(OH)_2$ is chemically unstable at high temperature and splits to form NiO and water molecule. The precipitated NiO nanocrystals so formed are:

$$Ni(OH_2) \rightarrow NiO + H_2O$$

Characterization methods

X-ray diffraction (XRD) analysis of the prepared nanomaterial was carried out by PANalytical diffractometer equipped with a CuKα monochromatic radiation (λ=1.5406 Å). SEI detector in the scanning electron microscopy (SEM) and an energy- dispersive X-ray spectroscopy (EDX) was used to analyze the morphology and chemical composition of the as- prepared NiO.

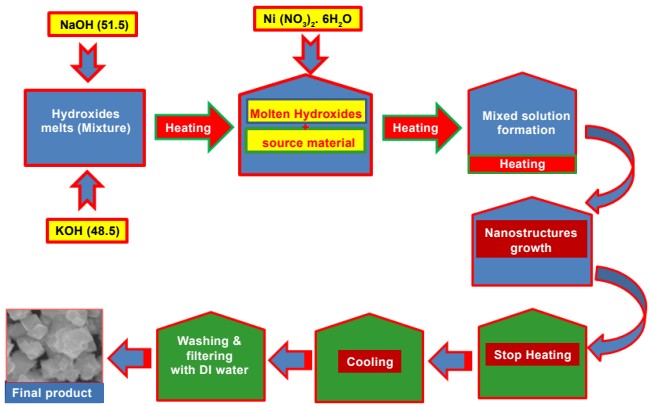

Figure 1: A general sketch of the procedure showing various steps involved in the CHM method for the preparation of NiO nanomaterial.

FTIR spectrum was studied on a Perkin Elmer FTIR spectrometer in the spectral range of 400-4000 cm^{-1}. The UV-visible absorption spectrum analysis was carried out in the spectral range 250 - 800 nm. The optical bandgap was estimated by using UV-visible absorption spectroscopy.

Results and Discussion

XRD analysis

The X-rays diffraction patterns of as- prepared samples of NiO nanostructures prepared at different temperatures; 180°C, 200°C, 220°C and 250°C are presented in Figure 2a. The sharp reflection peaks in the XRD patterns indicate the growth of nanosized crystallites of NiO (Bunsenite) nanostructures according to JCPDS# 00-071-1179, which crystallizes in the cubic structure. For the 180°C sample, the peak positions appearing at 2θ=37.25°, 43.27°, 62.85°, 74.96°, and 79.4° are corresponding to (111), (200), (220), (311) and (222) crystal planes respectively. All the reflections are indexed to face- centered cubic (FCC) of NiO phase with the lattice parameters a=b=c=0.41841 nm. The cubic structure NiO prepared at 200°C shows reflections at 2θ=37.16°, 43.18°, 62.68°, 75.16° and 79.15° for the (111), (200), (220), (311) and (222) orientations with lattice parameters a=b=c=0.41885 nm. Similar reflections are also observed for the samples prepared at 220°C and 250°C. The intensities of (111), (200) and (220) reflections are much stronger compared to other reflections in the XRD pattern. This gives strongly oriented crystallites in these planes directions. However, the growth along (200) is more prominent. The sharpness and strong intensity of these very certain peaks indicate a good crystalline nature of the product. The peak broadening in XRD pattern is a characteristic of the produced nanostructures. The average crystallite size of NiO is estimated by the well-known Debye-Sherrer formula using peak broadening [36],

$$D = K\lambda / \beta cos\theta \quad (1)$$

Here β denotes "full width at half maximum" of the diffraction peak in radian units, K is the correction factor and its value is assumed to be 0.94 for FWHM of the crystals, λ is the wavelength in unit of nm of Cu-Kα radiations and θ is the angular position in radian units (the Bragg's angle). The calculated values of crystallite sizes, corresponding to each plane along with FWHM are given in Table 1. The lattice parameter *a*, is calculated by the formula:

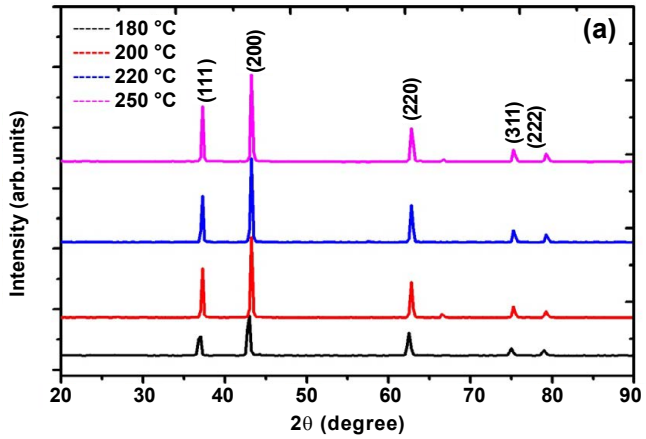

Figure 2a: X-ray diffraction pattern of NiO nanomaterial prepared at various temperatures in the range of 180-250°C for a constant processing time 24 h.

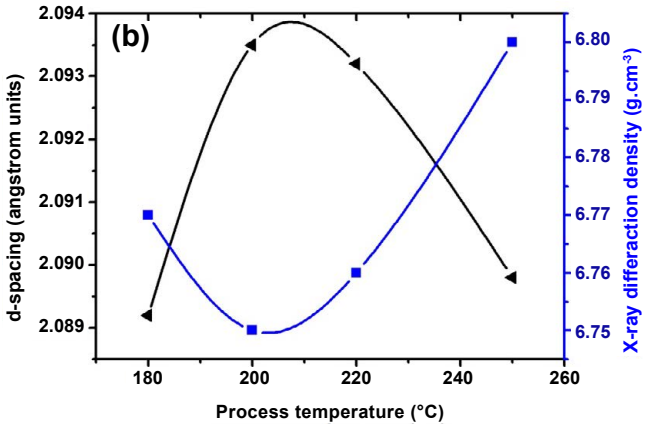

Figure 2b: Shows variation of the d-spacing and X-ray reflection density with process temperature.

$$\alpha = \frac{n\lambda}{2sin\theta\left(h^2 + k^2 + l^2\right)^{1/2}} \quad (2)$$

Then the cell volume of prepared cubic NiO nanostructures was estimated by the formula;

$$V_{cell} = a^3 \quad (3)$$

The *X*-ray density was calculated using molecular weight and volume of unit cell of the samples by the following formula [37];

$$\rho_{X-ray} = \frac{ZM}{V_{cell}N_A} \quad (4)$$

Where "Z" is the number of molecules per formula unit, "M" is the molar mass, "N_A" have its usual meanings and the V_{cell} is volume of a unit cell. All the calculated structural parameters are listed in the Table 1. It can be clearly seen that the lattice parameters have good agreement with the standard values. A small decrease is seen for the samples from 180°C to 220°C, where at 250°C the lattice parameter is very close to standard value. The cell volume also has the same tendency but values of the X-ray density has increased with processing temperature. The average size of crystallites obtained are; 23.71 nm (at 180°C), 30.81 nm (at 200°C), 31.01 nm (at 220°C), and 36.92 nm (at 250°C). The increase in crystallite size with rising reaction temperature is due to the viscosity of the hydroxide melts. As the viscosity of the hydroxide melts is greater at temperatures higher than 180°C, this causes slow nucleation and crystallization which result in formation of bigger nanosized crystallites. The variation in d-spacing and diffraction density with processing temperature are displayed in Figure 2b. The value of d-spacing shows an increasing trend in the temperature range 180-220°C followed by a reverse dropping trend at 250°C. Reflection density shows an opposite behavior to that observed for d-spacing in the same temperature range.

SEM characterization

Figures 3a and 3b shows SEM images and EDX of NiO nanomaterial prepared at different temperatures. These images give information on the morphology and composition of nanosized NiO. It seems that at temperatures 180°C and 200°C the prepared samples have no well- defined morphological structure. This predicts that a minimum temperature is required in the CHM process for different materials to starts to grow and nucleate in well- defined morphological peculiarities and structure. This also shows a temperature- dependent mechanism of nanomaterial synthesis by the CHM method. This temperature dependent nucleation can also be associated with the viscosity of the melts which is strongly influenced by the temperature factor and suggests viscosity is playing a significant role in the formation and growth of a nanomaterial in the CHM approach. As the temperature is raised to 220 and 250°C, a significant change is observed in the nanostructure of as- prepared samples. Interesting nanopyramid type structures are obtained with a high density. The color line circle in the image for 250°C shows two enclosed nanopyramids with its magnified marked image alongside EDS to manifests a clear visual picture of the

Processing Temperature	a (Å)	V (Å³)	Density (g.cm⁻³)	Crystallite size (nm)	Bandgap (eV)
180°C	4.1841	73.24	6.77	23.71	4.8
200°C	4.1885	73.48	6.75	30.81	4.5
220°C	4.1858	73.34	6.76	31.01	4.4
250°C	4.1791	72.99	6.8	36.92	4.0
NiO*	4.1780	72.93	6.803	-	4

Table 1: Structural and optical parameters of CHM prepared NiO calculated by XRD and absorption spectroscopy.

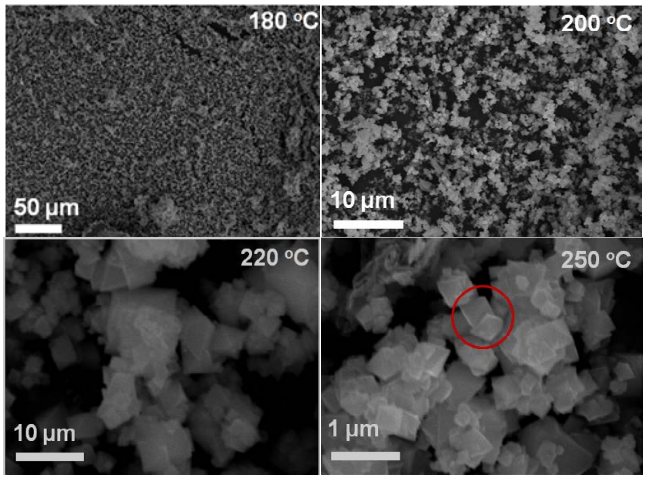

Figure 3a: SEM images of as- prepared NiO nanostructures at various temperatures (180, 200, 220, and 250°C).

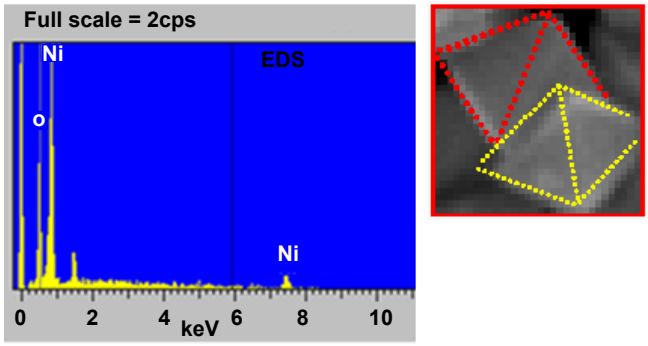

Figure 3b: EDS spectra taken on the sample showing Ni and O elements in the samples.

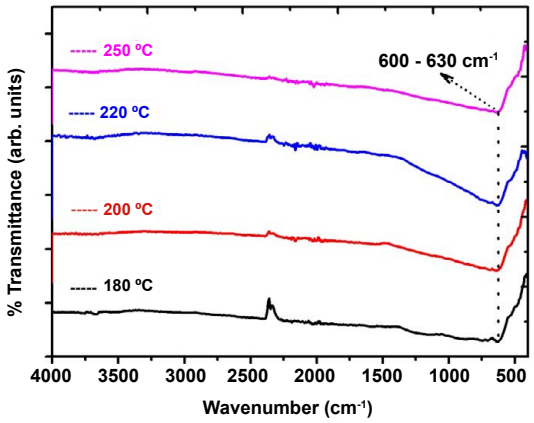

Figure 4: FT-IR spectra of NiO prepared at temperatures 180, 200, 220, and 250°C and for a constant reaction time (24 h).

prepared nanopyramids. The length of sides of these nanopyramids is in the range of 0.3–0.5 μm with random orientation. These NiO crystallites self-organized nanopyramids are high- density assemblies with a clear appearance. For the chemical composition, energy-dispersive X-ray (EDX) was performed on each sample and it was confirmed each sample showed the existence of Ni and O elements. This gives a strong signature on the chemically pure nature of the prepared product by the CHM method.

FTIR studies

The FTIR spectra were studied in the spectral range of 400-4000 cm^{-1} shown in Figure 4. FTIR is carried out in order to understand the chemical and structural roots of the prepared samples of NiO and the effects of reaction materials used. The absorption band in the region of 600–630 cm^{-1} is the characteristic stretching vibration band of NiO and is an obvious signature on the formation of NiO. The broadness of this band indicates the presence of NiO nanocrystals in the prepared samples. The observed vibration band for all the samples is well-consisted with the literature reported vibration band of NiO [38]. The small double peak at 2362 and 2346 cm^{-1} is caused by the presence of CO_2 molecules. The intensity of these bands decreases with increasing temperature [39,40]. FTIR study strongly supports the XRD results in respect of purity of the samples showing the formation of a single phase NiO.

UV- visible spectroscopy

This technique is based on the fact that an electron is moved from valence band to conduction band due to the absorbed photon having energy larger than the band gap energy of semiconductor. The electronic transition happened due to absorbed photon provides rich information about the type of transition. When the electron momentum is conserved the transition is direct otherwise indirect and energy of the transitions is measured using Tauc's relation [41,42].

UV-visible spectroscopy was performed to investigate the optical behavior of the nanostructures and to make an estimation of the bandgap. The optical absorption spectra of NiO samples at 180°C, 200°C, 220°C and 250°C were taken at room temperature by dispersing them in absolute ethanol which is a low absorption medium [43]. UV-vis absorption spectra of the samples are shown below in Figure 5a. A slight shift towards higher wavelength for the absorption edges was observed as the process temperature increased. This shift indicates a decrease in bandgap value, which can be attributed to an increase in the particle size. The value of absorption edges of NiO prepared at 180°C, 200°C, 220°C, 250°C were 295, 317, 321, 322 nanometer respectively. Also, it can be seen from the Figure 5 that there is an exponential decrease in the intensity of absorption with the increase in wavelength. This decreasing behavior in intensity is attributed for many semiconductors and may be due to many reasons similarly to internal electric fields within the crystal, deformation of lattice due to strain caused by imperfection and inelastic scattering of charge carriers by phonons [44]. Absorption coefficient (α) associated with the strong absorption region of the sample was calculated from the following relation [45]:

$$\alpha = 2.303 A/t \quad (5)$$

Here t' stands for the path length in cm and is taken to the cuvette length of 1 cm. According to the data of the absorption spectra, the optical bandgap (Eg) of NiO can be estimated by using the following Tauc equation [46]:

$$(\alpha h\upsilon)^n = B\left(h\upsilon - E_g\right) \quad (6)$$

Where hν is photo energy, α is absorption coefficient, B is a constant relative to the material and n is either 2 for direct band gap material or 1/2 for an indirect band gap material. According to the equation, the optical bandgap for the absorption peak can be obtained by extrapolating the linear portion of the $(\alpha h\nu)^n$ – hν curve to zero of the energy axis shown in Figure 5b. The corresponding bandgap

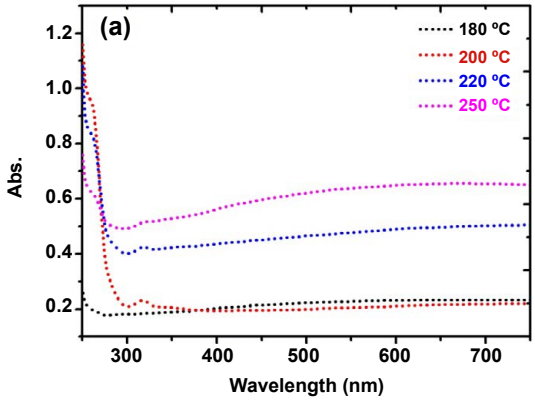

Figure 5a: UV- vis. absorption spectra of the CHM prepared NiO nanomaterial at various temperatures in the range of 180-250°C.

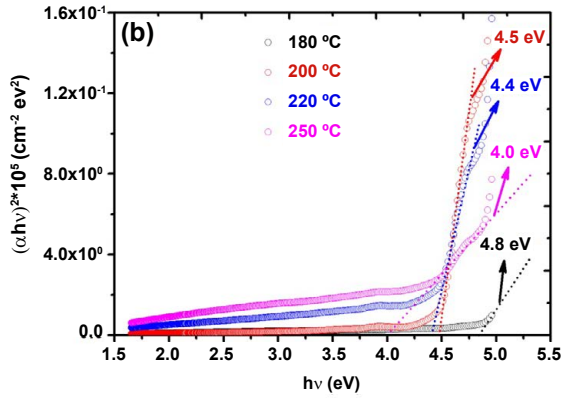

Figure 5b: The $(\alpha h\upsilon)^2$ vs. hυ plot of as prepared NiO. E_g is the intercept of the line at hν-axis for the bandgap calculation.

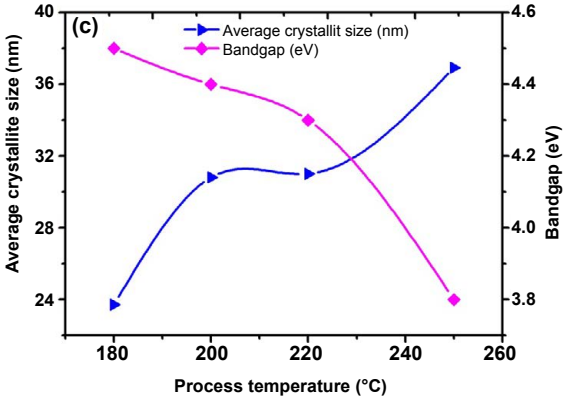

Figure 5c: Shows dependence of the average crystallite size and bandgap of NiO on the process temperature.

energies of produced nano-NiO at different temperature are given in Table 1. No linear relation was found for n = 1/2, suggesting that the as-synthesized NiO is semiconductor material with a direct transition at this energy [47]. The bandgap energies calculated are; 4.8 eV (at 180°C), 4.5 eV (at 200°C), 4.4 eV (220°C), and 4.0 eV (at 250°C). These values well consist reported by Khashan et al. [48] and Rifaya et al. [49]. This bandgap is the p-d character of NiO has been investigated by a range of spectroscopic techniques including optical absorption. The increasing trends of the bandgap energy upon the decreasing particles size can be associated nanosized structures. This effect is likely due to the chemical defects or vacancies present in the intergranular regions generating new energy level to reduce the band gap energy [50]. The NiO bandgap showed an increase with processing temperature with an overall maximum increased value up to 4.5 eV. The variation in E_g with processing temperature along with the crystallite size is depicted in Figure 5c.

Conclusion

In conclusion, pyramid- shaped NiO nanostructures were synthesized by using a low temperature and feasible CHM approach. A minimum limit on the processing temperature was established to nucleate NiO with a well- defined morphological structure. At temperatures below 220°C, NiO was presenting no definite morphology; while at temperatures in the range 220-250°C well-defined pyramid shaped morphological structures were obtained. The nanostructures were polycrystalline with an estimated average crystallite size in the range of 23.71 - 36.92 nm. The increase in average crystallite size assumed was caused by viscosity effect of the melts; playing a significant role in the nucleation process. Morphology showed a temperature dependent nature and was influenced by the processing temperature. The product was a pure crystalline material; composed of Ni and O elements with Ni-O stretching vibration bonding. The process temperature showed influence on the optical properties. The direct bandgap estimated was tuned in the range of 4.8-4.0 eV with the rise in process temperature. The present study would be beneficial as a new cost-effective route for the development of novel nanomaterials and temperature dependent morphological structures for prospective application in optoelectronics.

Acknowledgements

The research work carried-out in FUUAST. All the authors greatly acknowledge their parent institutes for this research work.

References

1. Thierry B, Majewski P, Ngothai Y, Shi Y (2007) Preparation of monodisperse functionalized nanoparticles. Internat J Nanotechnology 4: 5.
2. Jana NR, Chen YF, Peng XG (2004) Size- and shape-controlled magnetic (cr, mn, fe, co, ni) oxide nanocrystals via a simple and general approach. Chem Mater 16: 3931-3935.
3. Sasi B, Gopchandran KG, Manoj PK, Koshy P, Prabhakara Rao P (2002) Preparation of transparent and semiconducting NiO films. Vacuum 68: 149-154.
4. Thota S, Kumar J (2007) Sol-gel synthesis and anomalous magnetic behaviour of NiO nanoparticles. J Phys Chem Solids 68: 1951-1964.
5. Needham SA, Wang GX, Liu HK (2006) Synthesis of NiO nanotubes for use as negative electrodes in lithium ion batteries. J Power Sources 159: 254-257.
6. Chiu KF, Chang CY, Lin CM (2005) The electrochemical performance of bias-sputter deposited nanocrystalline nickel oxide thin films toward lithium. J Electrochem Soc 152: A1188-A1192.
7. Idirs NH, Wang JZ, Chou S, Zhong C, Rahman MM, et al. (2011) Effects of polypyrrole on the performance of nickel oxide anode materials for rechargeable lithium-ion batteries. Journal of Materials Research 26: 860-866.
8. Hotovy I, Huran J, Spiess L, Hascik S, Rehacek V (1999) Preparation of nickel oxide thin films for gas sensors applications. Sens Actuators B Chem 57: 147-152.
9. Bi H, Li S, Zhang, Du Y (2004) Ferromagnetic-like behavior of ultrafine NiO nanocrystallites. J Magn Magn Mater 277: 363-367.
10. Yoshito WK, Ussui V, Lazar DR, Paschoal JOA (2010) Synthesis of nickel oxide - zirconia composites by coprecipitation route followed by hydrothermal treatment. Material Science Forum 661: 977-982.
11. Marrero-Lopez DD, Ruiz-Morales JC, Pena-Martinez J, Canales-Vazques J, Nunez P (2008) Preparation of thin layer materials with macroporous microstructure for SOFC applications. J Solid State Chem 181: 685-692.
12. Richardson JR, Yiagas DI, Turk B, Forster K, Twigg MV (1991) Origin of superparamagnetism in nickel oxide. J Appl Phys 70: 6977-6982.
13. Lin SH, Chen FR, Kai JJ (2008) Electrochromic properties of nano-structured nickel oxide thin film prepared by spray pyrolysis method. Applied Surface Science 254: 2017-2022.
14. Borgstrom M, Blart E, Boschloo G, Mukhtar E, Hagfeldt A, et al. (2005) Sensitized hole injection of phosphorus porphyrin into NiO: toward new photovoltaic devices. J Phys Chem B 109: 22928-22934.
15. Chrissanthopoulos A, Baskoutas S, Bouroulos N, Dracopoulos V, Yannopoulos SN (2011) Synthesis and characterization of ZnO/NiO p–n heterojunctions: ZnO nanorods grown on NiO thin film by thermal evaporation. Photonics and Nanostructures-Fundamentals and Applications 9: 132-139.
16. Alejandre A, Medina F, Salagre P, Fabregat A, Sueiras JE (1998) Characterization and activity of copper and nickel catalysts for the oxidation of phenol aqueous solutions. Applied catalysis B 18: 307-315.

17. Dooley KM, Chen SY, Ross JRH (1994) Stable nickel-containing catalysts for the oxidative coupling of methane. J Catal 145: 402-408.

18. Zhang F, Zhou Y, Li H (2004) Nanocrystalline NiO as an electrode material for electrochemical capacitor. Mater Chem Phys 83: 260-264.

19. Bodurov G, Stefchev P, Ivanova T, Gesheva K (2014) Investigation of electrodeposited NiO films as electrochromic material for counter electrodes in Smart Windows. Mater Lett 117: 270-272.

20. Granqvist CG (1995) Handbook of inorganic electrochromic materials. Elsevier, Amsterdam.

21. Wang W, Liu Y, Xu C, Zheng C, Wang G (2002) Synthesis of NiO nanorods by a novel simple precursor thermal decomposition approach. Chem Phys Lett 362: 119-122.

22. Hosny NM (2011) Synthesis, characterization and optical band gap of NiO nanoparticles derived from anthranilic acid precursors via a thermal decomposition route. Polyhedron 30: 470-476.

23. Li X, Zhang X, Li Z, Qian Y (2006) Synthesis and characteristics of NiO nanoparticles by thermal decomposition of nickel dimethylglyoximate rods. Solid State Commun 137: 581-584.

24. Xiang L, Deng XY, Jin Y (2002) Experimental study on synthesis of NiO nano-particles. Scr Mater 47: 219-224.

25. Wang Y, Ke JJ (1996) Preparation of nickel oxide powder by decomposition of basic nickel carbonate in microwave field with nickel oxide seed as a microwave absorbing additive. Mater Res Bull 31: 55-61.

26. Anandan K, Rajendran V (2011) Morphological and size effects of NiO nanoparticles via solvothermal process and their optical properties. Solid State Electron 14: 43-47.

27. Wei Z, Qiao H, Yang H, Zhang C, Yan X (2009) Characterization of NiO nanoparticles by anodic arc plasma method. J Alloys Compd 479: 855-858.

28. Mohseni Meybodi S, Hosseini SA, Rezaee M, Sadrnezhaad SK, Mohammadyani D (2012) Synthesis of Wide Bandgap Nanocrystalline NiO Powder via a Sonochemical Method. Ultrason Sonochem 19: 841-845.

29. Deng XY, Chen Z (2004) Preparation of nano-NiO by ammonia precipitation and reaction in solution and competitive balance. Mater Lett 58: 276-280.

30. Hu C, Xi Y, Liu H, Wang ZL (2009) Composite-hydroxide-mediated approach as a general methodology for synthesizing nanostructures. Journal of Material Chemistry 19: 858-868.

31. Peng WQ, Cong GW, Qu SC, Wang ZG (2005) Synthesis of shuttle-like ZnO nanostructures from precursor ZnS nanoparticles. Nanotechnology 16: 1469.

32. Khan TM, Shahid T, Zakria M, Shakoor RI (2015) Optoelectronic properties and temperature dependent mechanisms of CHM approach for the synthesis of CdO nanomaterials. Electron Mater Lett 11: 366-373.

33. Khan TM, Zakria M, Shakoor RI, Ahmad M, Raffi M (2015) Mechanisms of composite-hydroxide-mediated approach for the synthesis of functional ZnO nanostructures and morphological dependent optical emissions. Advanced Materials Letters 6: 592-599.

34. Shahid T, Arfan M, Ahmad W, BiBi T, Khan TM (2016) Synthesis and doping feasibility of composite-hydroxide-mediated approach for the $Cu_{1-x}Zn_xO$ nanomaterials. Advanced Materials Letters 7: 561-566.

35. An C, Wang R, Wang S, Liu Y (2008) A low temperature composite-hydroxide approach to NiO nanocrystals. Mater Res Bull 43: 2563-2568.

36. Abdeen AM, Hemeda OM, Assem EE, Elsehly MM (2002) Structural, electrical and transport phenomena of Co ferrite substituted by Cd. J Magn Magn Mater 238: 75-83.

37. Anandan K, Rajendran V (2011) Morphological and size effects of NiO nanoparticles via solvothermal process and their optical properties. Mater Sci Semicond Process 14: 43-47.

38. El-Kemary M, Nagy N, El-Mehasseb I (2013) Nickel oxide nanoparticles: Synthesis and spectral studies of interactions with glucose. Materials Science in Semiconductor Processing 16: 1747-1752.

39. Snopatin GE, Yu M, Matveeva M, Butsyn GG (2006) Effect of SO_2 impurity on the optical transmission of As_2S_3 glass. Inorg Mater 42: 1388-1392.

40. Willardson R, Beer A (1967) Optical Properties of III-V Compounds. Academic Press, New York. pp: 318-400.

41. Dressel M, Gruner G (2002) Electrodynamics of solids optical properties of electron in matter. Cambridge University Press, USA.

42. Dharmaraj N, Prabu P, Nagarajan S, Kim CH, Park JH, et al. (2006) Synthesis of nickel oxide nanoparticles using nickel acetate and poly(vinyl acetate) precursor. Mater Sci Eng B 128: 111-114.

43. Mallick P, Sahoo CS, Mishra NC (2012) Structural and optical characterization of NiO nanoparticles synthesized by sol-gel route. AIP Conf Proc 1461: 229-232.

44. Kumar H, Rani R (2013) Structural and optical characterization of ZnO nanoparticles synthesized by microemulsion route. Int Lett Chem Phys Astron 14: 26-36.

45. Tauc J (1966) Optical properties of solids. Academic Press Inc., New York.

46. Hwang SS, Vasiliev AL, Padture NP (2007) Improved processing and oxidation-resistance of ZrB2 ultra-high temperature ceramics containing SiC nanodispersoids. Mater Sci Eng A 464: 216-224.

47. Khashan KS, Sulaiman GM, Ameer FAKA, Napolitano G (2016) Synthesis, characterization and antibacterial activity of colloidal NiO Nanoparticles. Pak J Pharm Sci 29: 541-546.

48. Tasker PW (1979) The stability of ionic crystal surfaces. J Phys C: Solid State Phys 12: 4977-4984.

49. Nowsath Rifaya M, Theivasanthi T, Alagar M (2012) Chemical capping synthesis of nickel oxide nanoparticles and their characterizations studies. Nanoscience and Nanotechnology 2: 134-138.

50. Song X, Gao L (2008) Facile synthesis of polycrystalline NiO nanorods assisted by microwave heating. J Am Ceram Soc 91: 3465-3468.